World Applied Sciences Journal 28 (12): 1888-1895, 2013
ISSN 1818-4952
© IDOSI Publications, 2013
DOI: 10.5829/idosi.wasj.2013.28.12.1669

# Hydromagnetic Flow of Micropolar Fluid between two Horizontal Plates, both the Plates being Stretching Sheets

[1]Sajjad Hussain, [2]M. Anwar Kamal and [3]M. Shafique

[1]Centre for Advanced Studies in Pure and Applied Mathematics, B.Z. University, Multan, Pakistan
[2]Department of Mathematics, Suleman Bin Abdul Aziz Uni., Saudi Arabia
[3]Department of Mathematics, Gomal University, D.I. Khan, Pakistan

**Abstract:** Hydromaganetic flow of micropolar fluid between two horizontal parallel plates, the lower is a stretching sheet and the upper one is a porous stretching sheet. The flow is in the presence of a transverse magnetic field is studied numerically. The effects of transverse magnetic field parameter M, Reynolds number R and suction parameter $\lambda$ on the velocity and microrotation fields have been observed. The governing partial differential equations of motion are transformed to ordinary differential form by using appropriate similarity transformations. The resulting equations of motion are solved numerically using SOR method and Simpson's (1/3) Rule. The numerical results have been improved by using Richardson extrapolation to the limit.

**Key words:** Micropolar fluids . hyderomagnetic flow . reynolds number . similarity transformations . richardson extrapolation

## INTRODUCTION

The theory of micropolar fluids first proposed by Eringen [1, 2] includes the effects of local rotary inertia and couple stresses. These fluids consist of dumb-bell or short rigid cylindrical elements. The presence of smoke or dust particularly in a gas may also be modeled using micropolar fluid dynamics. Several researchers are engaged in studying various phenomena of micropolar fluid flow. In extrusion processes, the fluid flow due to a stretching surface has its own importance. Kamal and Sifat β] studied 3-dimensional micropolar fluid motion caused by the stretching surface. Shafique and Rashid [4] obtained numerical solution of three dimensional micropolar fluid flows due to a stretching flat surface. Magnetic effect in fluid dynamics is considered important because of its role in many industrial applications. Flow of an electrically conducting non- Newtonian fluid past a stretching surface was studied by Able *et al*. [5] when a uniform magnetic field acts transverse to the surface. MHD flow due to non coaxial rotations of an accelerated disk and a fluid at infinity was analyzed by Asghar *et al*. [6]. MHD flow of micropolar fluid past a stretching sheet with heat transfer and with suction/blowing through a porous medium has been studied by Eldabe *et al*. [7]. Ishak *et al*. [8] investigated magnetohderodynamic flow of micropolar fluid towards a stagnation point on a vertical surface. MHD flow of micropolar fluid near a stagnation point towards a non linear stretching surface has been examined by Hayat *et al*. [9]. The fluid flows over a permeable surface have numerous applications, for example for control of boundary layer separation with suction or injection. Sastry and Rao [10] studied the effects of suction parameter on laminar micropolar fluid in a porous channel. Ashraf *et al*. [11] obtained numerical simulation for two dimensional flow of a micropolar fluid between an impermeable and a permeable disk. Guram and Anwar [12] considered the steady, laminar and incompressible flow of a micropolar fluid due to a rotating disk with suction and injection. Ashraf *et al*. [13] presented numerical study for the steady, two-dimensional, laminar and incompressible flow of a micropolar fluid in a porous channel.

In the present study, numerical results have been obtained for hydromagnetic flow of micropolar fluid between two horizontal parallel plates when the lower one is a stretching sheet and the upper one is a porous stretching sheet. The flow is in the presence of a transverse magnetic field. The effects of transverse magnetic field parameter M and suction parameter $\lambda$ and Reynolds number R are studied on the velocity field and microrotation under two situations namely either both the plates are being stretching sheets or only the lower plate is stretching. The results are computed

**Corresponding Author:** Sajjad Hussain, Centre for Advanced Studies in Pure and Applied Mathematics, B.Z. University, Multan, Pakistan

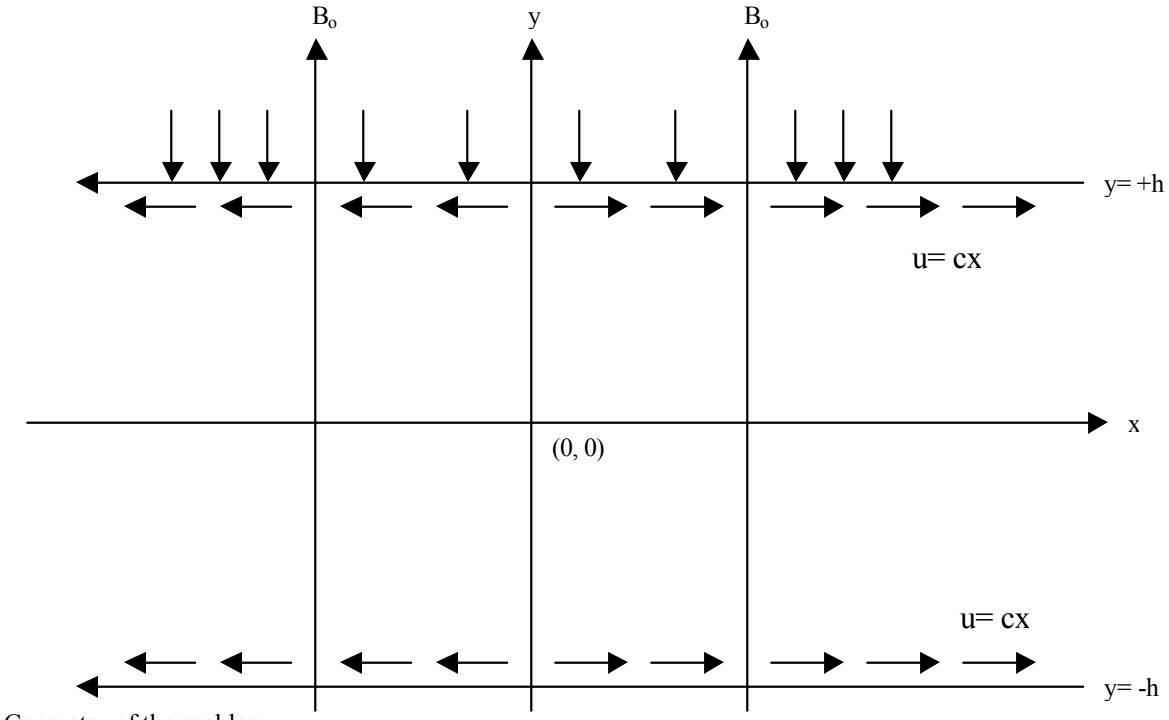


Geometry of the problem

for different values of the parameters in the range $1 \le M \le 4$, $0.05 \le R \le 0.8$ and $1 \le \lambda \le 3$. Dash and Tripathy [14] studied this problem for Newtonian fluids for ranges of flow parameters M =1.0, 3.0, $\lambda$ = 1.0, 3.0 and R=0.05, 0.20. The present results for micropolar fluid have been compared with the previous results. The results are in good agreement. The section 2 presents mathematical analysis. The finite difference equations are given in section 3. The details of computational procedure are provided in section 4. The results of the present study are discussed in tabular as well as graphical form in section 5. Tables and graphs are presented in section 6.

## MATHEMATICAL ANALYSIS

In order to formulate the problem, it is assumed that the fluid is viscous and electrically conducting. The fluid flow is steady, incompressible and between two horizontal, parallel, non conducting plates. The lower plate is a stretching sheet and the upper one is a porous stretching sheet. Cartesian coordinate system is used where the y-axis is perpendicular to the plates located at y = h, y = -h. Two equal and opposite forces are introduced to stretch the lower and the upper plates in a way that the position of the points (0, h), (0, -h) remains unchanged. The fluid with constant velocity $V_0$ is injected through the upper porous plate. This flow is considered in the presence of a transverse magnetic field. The body couple is absent.

Under the above assumptions the basic equations of motion for micropolar fluids, formulated by Eringen [2] become:

$$\nabla \underline{V} = 0 \tag{1}$$

$$\begin{aligned} &-(\mu + \kappa)\nabla \times (\nabla \times \underline{\mathbf{V}}) + \kappa(\nabla \times \underline{\upsilon}) \\ &-\nabla p + \underline{J} \times \underline{B} = \rho \left( \underline{\mathbf{V}} \cdot \nabla \right) \underline{V} \end{aligned} \tag{2}$$

$$-\gamma \left( \nabla \times \nabla \times \underline{\upsilon} \right) + \kappa(\nabla \times \underline{\mathbf{V}}) - 2\kappa \underline{\upsilon} = \rho j \left( \underline{\mathbf{V}} \cdot \nabla \right) \underline{\upsilon} \tag{3}$$

where $\underline{V}$ is velocity and $\underline{\upsilon}$ is microrotation vector, p is pressure, $\rho$ is density and $\underline{J} \times \underline{B}$ is the electromagnetic body force with $\underline{J}$ the current density. $\underline{B}$ is the total magnetic field strength. The induced magnetic field is neglected because the magnetic Reynolds number is small. It is considered that the external electric field is zero and the electric field due to polarization of charges is negligible which implies that $\underline{E}$ = 0. Under this consideration the electromagnetic body force takes the form [15] as:

$$\underline{J} \times \underline{B} = \sigma(\underline{V} \times \underline{B}) \times \underline{B} = -\sigma B^2 \underline{V} \tag{4}$$

The associated boundary conditions are:

$$u = cx, v = 0, \underline{\upsilon} = 0$$

at y = -h, c>0

$$u = cx, v = V_0, \upsilon = 0$$

at

$$y = h,\ c>0 \tag{5}$$

Now, using similarity transformations:

$$u = cxf'(\eta), v = -chf(\eta), \upsilon_3 = -\frac{cx}{h}L(\eta) \tag{6}$$

where $\eta = y/h$ is dimensionless variable.

The continuity equation (1) is identically satisfied and the equation (2) leads to:

$$(2ff' - ff' - ff''' - \frac{1}{R}f'''' + \frac{M^2}{R}f'') + \frac{\kappa}{\rho ch^2}L' = 0 \tag{7}$$

where primes denote differentiation with respect to $\eta$
Integrating equation (7) with respect to $\eta$

$$f''' - R\left(f'^2 - ff'' + C_1L'\right) - M^2f' = \beta \tag{8}$$

The equation (3) yields:

$$L' + C_2ff'' - 2C_2L = C_3(fL' - fL) \tag{9}$$

where $\beta$ is constant of integration and $C_1$, $C_2$, $C_3$ are non dimensional constants:

The corresponding boundary conditions (4) become:

$$f(-1) = 0, f'(-1) = 1, L(-1) = 0, f(1) = \lambda, f'(1) = 1, L(1) = 0 \tag{10}$$

where

$$R = \frac{ch^2}{\nu}, M = \sqrt{\sigma/\rho\nu}B_0h$$

and $\lambda = V_0/ch$ is suction parameter.

## FINITE-DIFFERENCE EQUATIONS:

Let

$$f' = q \tag{11}$$

Then equations (8) and (9) become

$$q'' - R(q^2 - fq' + c_1L') - M^2q = \beta \tag{12}$$

$$L' + c_2q' - 2c_2L = c_3(fL' - fL) \tag{13}$$

By using central difference approximations at a typical point $\eta = \eta_n$ of the interval $[0,\infty)$ equation (12) and (13) by and obtain

$$\begin{aligned}&(2 + hRq_n)q_{n+1} - (4 + 2h^2M^2 + 2h^2Rq_n)q_n + \\ &(2 - hRq_n)q_{n-1} - c_1hR\left(L_{n+1} - L_{n-1}\right) - 2h^2\beta = 0\end{aligned} \tag{14}$$

$$\begin{aligned}&(2 - c_3hf_n)L_{n+1} - (4 + 2c_2h^2 - 2c_3h^2q_n)L_n \\ &+(2 + c_3hf_n)L_{n-1} + c_2h(q_{n+1} - q_{n-1}) = 0\end{aligned} \tag{15}$$

where h denotes grid size. The equation (11) is integrated numerically. Also the symbols used denote $q_n = q(\eta_n)$ and $L_n = L(\eta_n)$. The interval $[0,\infty)$ is replaced by [0, b] for computational purposes, where b is a sufficiently large.

## COMPUTATIONAL PROCEDURE

The finite difference equations (14) and (15) and the first order ordinary differential equation (11) are solved simultaneously by using SOR method Smith [16] and Simpson's (1/3) rule Gerald [17] with the formula given in Milne [18] respectively subject to the appropriate boundary conditions.

The order of the sequence of iterations is as follows:

1. The equations (14) and (15) for the solution of q and L are solved subject to the following boundary conditions:

   $f = 0$, q = 1, L = 0 When $\eta$ = -1

   $f = \lambda$, q = 1, L = 0 When $\eta$ = 1

2. For the solution of $f$ we use the computed values of q from above step in to equations (11) and integrate by Simpson's (1/3) rule.
3. The optimum value of the relaxation parameter $\omega_{opt}$ is estimated to accelerate the convergence of the SOR method.
4. The SOR procedure is terminated when the following criterion is satisfied for q and L:

$$\max_{i=1}^{n}\left|U_i^{n+1} - U_i^n\right| < 10^{-6}$$

where n denotes the number of iterations and U stands for each of q and L.

The above steps 1 to 4 are repeated for higher grid levels h/2 and h/4. The SOR procedure gives the

solution of q and L of order of accuracy $O(h^2)$ due to second order finite differences approximations used for derivatives. While the Simpson's (1/3) rule gives the order of accuracy $O(h^5)$ in the solution of f. The higher order accuracy $O(h^6)$ in the solution of $f'$ on the basis of above solutions is achieved by using Richardson's Extrapolation Method Burden [19].

## NUMERICAL RESULTS AND DISCUSSION

The numerical results have been computed for several values of flow parameters namely λ, R and M in the ranges mentioned above. The effect of these parameters have been studied on the $f'$, f and L for the cases given in following table.

| Cases | $C_1$ | $C_2$ | $C_3$ |
|---|---|---|---|
| I | 1.0 | 2.0 | 3.0 |
| II | 1.5 | 2.5 | 3.5 |
| III | 0.1 | 0.2 | 0.3 |
| IV | 5.0 | 4.0 | 3.0 |

In order to check the accuracy of the numerical results, they have been computed and compared using three different grid sizes namely h=0.2, 0.1 and 0.05. The Table 4 contains the results of $f'$,$f$ and L for some values of the parameters λ, R and M in the case-II when both the plates are being stretching sheet. Table 5 gives the results of $f'$,$f$ and L for some values of the parameters λ, R and M in the case-II when the lower plate is a stretching sheet. The results for velocity component $f'$ are given in higher order accuracy $O(h^6)$ in the Table 1-3 for Case-III of non-dimensional material constants. The comparison between results of micropolar fluid and Newtonian fluid for some values of flow parameters λ,R and M is given in the Table 6. The values for micropolar fluid and Newtonian fluid placed in this table are those which are calculated on the finer grid size.

The graphical pattern of the results shows that the velocity field is almost symmetric about the centre of the channel $\eta = 0$ when both the plates are being stretched at the same rate but it is not the case with the stretching of the lower plate only as depicted in Fig. 1-3. It has been noted that $f'$ increases in the lower half of the channel for increasing R and decreases in the upper half of the channel. This effect can be observed in Fig. 2. It can be observed that an increase in the value of R increases f at all points, this component of velocity increases with increase of η when M is constant as depicted in Fig. 4 and 5.

The effect of λ is maximum on the primary flow $f'$ at the center of the channel for fixed values of M. Also this effect is same, either both the sheets being stretched or the single sheet being stretched. Detailed comparison, both tabular and graphical for $\lambda = 1$and $\lambda = 3$ shows that the suction parameter radically changes the primary flow velocity $f'$ but the value of f increases with the increase of λ when M is constant. This can be observed in tables and figures particularly in Fig. 4 and 5. The Fig. 3 and 2 show that when $\lambda = 1$, the Lorentz force decreases $f'$ near the lower plate and increases it near the upper plate. Figure 4 and 5 show that when λ is constant, the Lorentz force decreases f with the increase in the magnetic field strength.

Figure 6 and 7 show the comparison of micropolar and Newtonian fluids. Figure 8 and 9 depict microrotation field when both the plates are being stretching sheets. Figure 10 demonstrates the microrotation field when the lower plate is being stretching sheet. The results for these graphs have been calculated in case- IV of the non dimensional material constants.

Table 1: M = 1.0, λ = 1.0, R = 0.05 M = 4.0, λ = 1.0, R = 0.05

| Numerical results using richardson extrapolation method | | | | | | | | | |
|---|---|---|---|---|---|---|---|---|---|
| h = 0.2 h = 0.1 h = 0.05 extrapolated | | | | | h = 0.2 h = 0.1 h = 0.05 extrapolated | | | | |
| η | $f'$ | $f'$ | $f'$ | $f'$ | η | $f'$ | $f'$ | $f'$ | $f'$ |
| 0.0 | 1.000000 | 1.000000 | 1.000000 | 1.000000 | 0.0 | 1.000000 | 1.000000 | 1.000000 | 1.000000 |
| 0.2 | 0.719477 | 0.718947 | 0.718813 | 0.718768 | 0.2 | 0.638627 | 0.634118 | 0.632929 | 0.632528 |
| 0.4 | 0.512920 | 0.512029 | 0.511804 | 0.511728 | 0.4 | 0.473828 | 0.469649 | 0.468560 | 0.468193 |
| 0.6 | 0.371658 | 0.370536 | 0.370251 | 0.370156 | 0.6 | 0.399673 | 0.396646 | 0.395866 | 0.395603 |
| 0.8 | 0.289713 | 0.288461 | 0.288143 | 0.288037 | 0.8 | 0.368442 | 0.366252 | 0.365693 | 0.365506 |
| 1.0 | 0.263517 | 0.262223 | 0.261895 | 0.261785 | 1.0 | 0.360001 | 0.358092 | 0.357606 | 0.357444 |
| 1.2 | 0.291750 | 0.290497 | 0.290180 | 0.290074 | 1.2 | 0.368848 | 0.366637 | 0.366072 | 0.365883 |
| 1.4 | 0.375266 | 0.374142 | 0.373859 | 0.373764 | 1.4 | 0.400543 | 0.397478 | 0.396687 | 0.396420 |
| 1.6 | 0.517127 | 0.516235 | 0.516010 | 0.515935 | 1.6 | 0.475188 | 0.470965 | 0.469862 | 0.469490 |
| 1.8 | 0.722722 | 0.722191 | 0.722058 | 0.722013 | 1.8 | 0.640144 | 0.635604 | 0.634406 | 0.634002 |
| 2.0 | 1.000000 | 1.000000 | 1.000000 | 1.000000 | 2.0 | 1.000000 | 1.000000 | 1.000000 | 1.000000 |

Table 2: M = 3.0, λ = 3.0, R = 0.05 M = 3.0, λ = 3.0, R = 0.2

| Numerical results using richardson extrapolation method | | | | | | | | | |
|---|---|---|---|---|---|---|---|---|---|
| h = 0.2 h = 0.1 h = 0.05 extrapolated | | | | | h = 0.2 h = 0.1 h = 0.05 extrapolated | | | | |
| η | $f'$ | $f'$ | $f'$ | $f'$ | η | $f'$ | $f'$ | $f'$ | $f'$ |
| 0.0 | 1.000000 | 1.000000 | 1.000000 | 1.000000 | 0.0 | 1.000000 | 1.000000 | 1.000000 | 1.000000 |
| 0.2 | 1.334079 | 1.336860 | 1.337577 | 1.337818 | 0.2 | 1.341432 | 1.344195 | 1.344924 | 1.345170 |
| 0.4 | 1.516061 | 1.519254 | 1.520073 | 1.520347 | 0.4 | 1.524668 | 1.527782 | 1.528606 | 1.528884 |
| 0.6 | 1.612371 | 1.615253 | 1.615994 | 1.616242 | 0.6 | 1.619411 | 1.622183 | 1.622914 | 1.623161 |
| 0.8 | 1.658410 | 1.660955 | 1.661601 | 1.661818 | 0.8 | 1.662730 | 1.665166 | 1.665803 | 1.666017 |
| 1.0 | 1.671304 | 1.673725 | 1.674338 | 1.674543 | 1.0 | 1.672433 | 1.674779 | 1.675383 | 1.675586 |
| 1.2 | 1.656138 | 1.658710 | 1.659363 | 1.659582 | 1.2 | 1.653774 | 1.656319 | 1.656963 | 1.657179 |
| 1.4 | 1.607915 | 1.610843 | 1.611590 | 1.611841 | 1.4 | 1.601860 | 1.604798 | 1.605537 | 1.605784 |
| 1.6 | 1.509957 | 1.513184 | 1.514010 | 1.514287 | 1.6 | 1.500687 | 1.503922 | 1.504736 | 1.505008 |
| 1.8 | 1.328271 | 1.331056 | 1.331773 | 1.332013 | 1.8 | 1.318723 | 1.321478 | 1.322175 | 1.322408 |
| 2.0 | 1.000000 | 1.000000 | 1.000000 | 1.000000 | 2.0 | 1.000000 | 1.000000 | 1.000000 | 1.000000 |

Table 3: M=4.0, λ = 3.0, R=0.1 M=4.0, λ=3.0, R=0.8

| Numerical results using richardson extrapolation method | | | | | | | | | |
|---|---|---|---|---|---|---|---|---|---|
| h = 0.2 h = 0.1 h = 0.05 extrapolated | | | | | h = 0.2 h = 0.1 h = 0.05 extrapolated | | | | |
| η | $f'$ | $f'$ | $f'$ | $f'$ | η | $f'$ | $f'$ | $f'$ | $f'$ |
| 0.0 | 1.000000 | 1.000000 | 1.000000 | 1.000000 | 0.0 | 1.000000 | 1.000000 | 1.000000 | 1.000000 |
| 0.2 | 1.364167 | 1.368668 | 1.369858 | 1.370261 | 0.2 | 1.387914 | 1.392277 | 1.393441 | 1.393835 |
| 0.4 | 1.529252 | 1.533385 | 1.534471 | 1.534837 | 0.4 | 1.554395 | 1.558082 | 1.559060 | 1.559391 |
| 0.6 | 1.602806 | 1.605777 | 1.606548 | 1.606808 | 0.6 | 1.622208 | 1.624676 | 1.625325 | 1.625544 |
| 0.8 | 1.633209 | 1.635357 | 1.635909 | 1.636095 | 0.8 | 1.645459 | 1.647276 | 1.647749 | 1.647908 |
| 1.0 | 1.640743 | 1.642645 | 1.643131 | 1.643294 | 1.0 | 1.645476 | 1.647329 | 1.647807 | 1.647968 |
| 1.2 | 1.630806 | 1.633053 | 1.633629 | 1.633822 | 1.2 | 1.626734 | 1.629212 | 1.629850 | 1.630065 |
| 1.4 | 1.597658 | 1.600799 | 1.601609 | 1.601882 | 1.4 | 1.582316 | 1.585830 | 1.586740 | 1.587047 |
| 1.6 | 1.521224 | 1.525534 | 1.526657 | 1.527036 | 1.6 | 1.493075 | 1.497601 | 1.498782 | 1.499181 |
| 1.8 | 1.355253 | 1.359829 | 1.361034 | 1.361441 | 1.8 | 1.321609 | 1.325925 | 1.327061 | 1.327445 |
| 2.0 | 1.000000 | 1.000000 | 1.000000 | 1.000000 | 2.0 | 1.000000 | 1.000000 | 1.000000 | 1.000000 |

Table 4: M = 3.0, λ = 1.0, R = 0.05 M = 4.0, λ = 1.0, R = 0.05

| Numerical results using SOR method and Simpson's rule on finer grid size | | | | | | | |
|---|---|---|---|---|---|---|---|
| η | $f$ | $f'$ | L | η | $f$ | $f'$ | L |
| 0.0 | 0.000000 | 1.000000 | 0.000000 | 0.0 | 0.000000 | 1.000000 | 0.000000 |
| 0.2 | 0.163137 | 0.664774 | -0.169069 | 0.2 | 0.158706 | 0.634736 | -0.158091 |
| 0.4 | 0.275961 | 0.482078 | -0.223569 | 0.4 | 0.266999 | 0.469858 | -0.199134 |
| 0.6 | 0.361615 | 0.385075 | -0.220719 | 0.6 | 0.352625 | 0.396365 | -0.191577 |
| 0.8 | 0.433293 | 0.338203 | -0.187580 | 0.8 | 0.428338 | 0.365591 | -0.162368 |
| 1.0 | 0.499066 | 0.324273 | -0.136180 | 1.0 | 0.500323 | 0.357162 | -0.120787 |
| 1.2 | 0.564839 | 0.338216 | -0.071623 | 1.2 | 0.572302 | 0.365545 | -0.068709 |
| 1.4 | 0.636530 | 0.385213 | 0.001982 | 1.4 | 0.648009 | 0.396383 | -0.006374 |
| 1.6 | 0.722240 | 0.482517 | 0.073501 | 1.6 | 0.733663 | 0.470149 | 0.060086 |
| 1.8 | 0.835186 | 0.665516 | 0.107499 | 1.8 | 0.842053 | 0.635401 | 0.099633 |
| 2.0 | 0.998433 | 1.000000 | 0.000000 | 2.0 | 1.000866 | 1.000000 | 0.000000 |

Table 5: M=1.0, λ=1.0, R=0.30 M=3.0, λ=1.0, R=0.30

| Numerical results using SOR method and Simpson's rule on finer grid size | | | | | | | |
|---|---|---|---|---|---|---|---|
| η | $f$ | $f'$ | L | η | $f$ | $f'$ | L |
| 0.0 | 0.000000 | 1.000000 | 0.000000 | 0.0 | 0.000000 | 1.000000 | 0.000000 |
| 0.2 | 0.189034 | 0.891769 | -0.147745 | 0.2 | 0.175726 | 0.778394 | -0.144944 |
| 0.4 | 0.357222 | 0.791232 | -0.255925 | 0.4 | 0.317739 | 0.653523 | -0.215735 |
| 0.6 | 0.505900 | 0.696270 | -0.335481 | 0.6 | 0.440643 | 0.581849 | -0.251253 |
| 0.8 | 0.635935 | 0.604369 | -0.393150 | 0.8 | 0.552291 | 0.537655 | -0.271172 |
| 1.0 | 0.747673 | 0.512862 | -0.432411 | 1.0 | 0.656442 | 0.504649 | -0.285297 |
| 1.2 | 0.840931 | 0.419135 | -0.453270 | 1.2 | 0.754078 | 0.470552 | -0.297442 |
| 1.4 | 0.915026 | 0.320921 | -0.450410 | 1.4 | 0.843780 | 0.423088 | -0.305426 |
| 1.6 | 0.968905 | 0.216870 | -0.408109 | 1.6 | 0.921377 | 0.346347 | -0.296043 |
| 1.8 | 1.001433 | 0.107855 | -0.287917 | 1.8 | 0.978833 | 0.216924 | -0.229666 |
| 2.0 | 1.012100 | 0.000000 | 0.000000 | 2.0 | 1.002345 | 0.000000 | 0.000000 |

Table 6: Comparison table for micropolar and Newtonian fluids (case-III)

| η | R | M | λ | β | Micropolar $f'$ | Newtonian $f'$ |
|---|---|---|---|---|---|---|
| 1.0 | 0.05 | 1.0 | 1.0 | 1.093626 | 0.261895 | 0.261939 |
| 1.0 | 0.05 | 3.0 | 1.0 | -2.267975 | 0.325996 | 0.326008 |
| 1.0 | 0.20 | 3.0 | 3.0 | -16.326400 | 1.675383 | 1.675328 |
| 1.0 | 0.40 | 2.0 | 1.0 | -0.168730 | 0.291246 | 0.291429 |
| 1.0 | 0.40 | 4.0 | 1.0 | -5.365580 | 0.357007 | 0.357061 |
| 1.0 | 0.40 | 2.0 | 3.0 | -9.081195 | 1.699496 | 1.709340 |
| 1.0 | 0.80 | 2.0 | 3.0 | -10.332480 | 1.707297 | 1.707032 |
| 1.0 | 0.80 | 4.0 | 3.0 | -29.016950 | 1.647807 | 1.647703 |

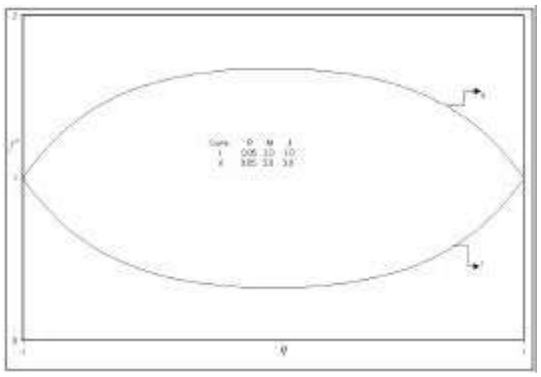

Fig. 1: Graph of $f'$ when both the plates are stretching sheets

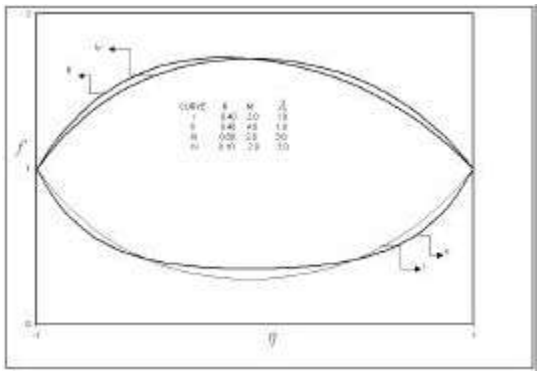

Fig. 2: Graph of $f'$ when both the plates are stretching sheets

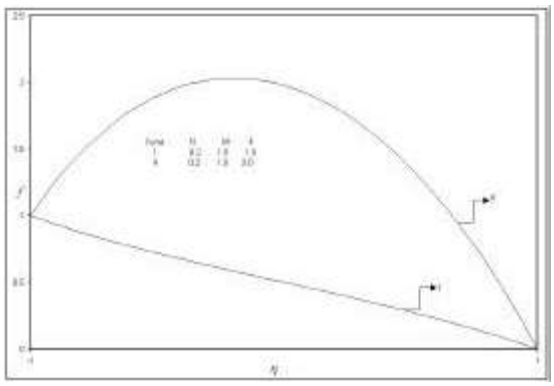

Fig. 3: Graph of $f'$ when the lower plate is a stretching sheet

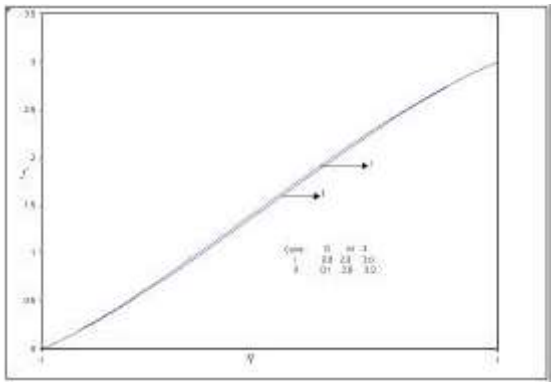

Fig. 4: Graph of transverse velocity f

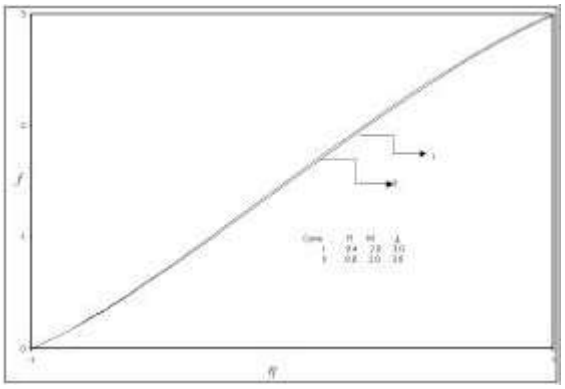

Fig. 5: Graph of transverse velocity f

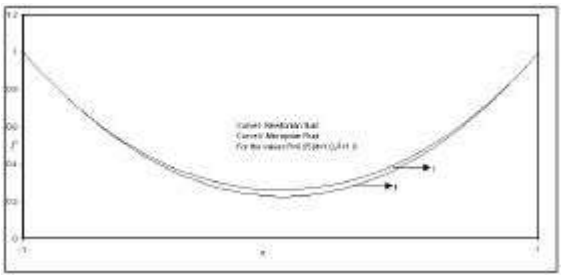

Fig. 6: Graph of $f'$ for the comparison of Newtonian and micropolar fluid flow when both the plates are stretching sheets

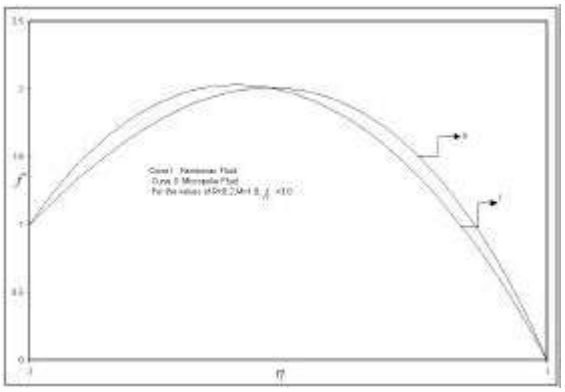

Fig. 7: Graph of $f'$ for the comparison of Newtonian and micropolar fluid flow when both the plates are stretching sheets

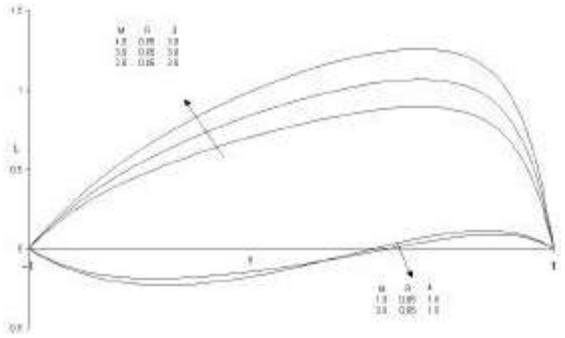

Fig. 8: Graph of microrotation L when both the plates are stretching sheets

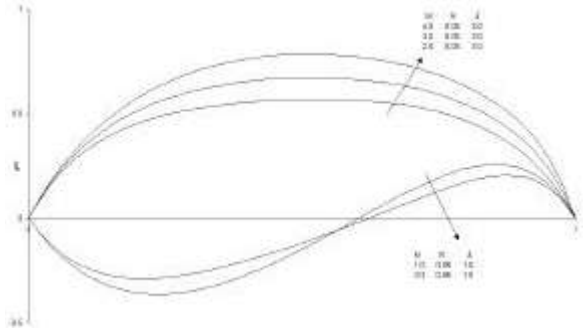

Fig. 9: Graph of microrotation L when both the plates are stretching sheets

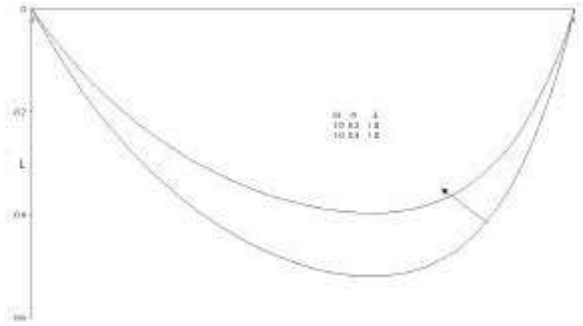

Fig. 10: Graph of microrotation L when the lower plate is a stretching sheet

## REFERENCES


1. Eringen, A.C., 1964. Simple microfluids. Int. J. Eng. Sci., 2 (2): 205-217.
2. Eringen, A.C., 1966. Theory of micropolar fluids. J. Math. Mech., 16 (1): 1-18.
3. Kamal, M.A. and S. Hussain, 1994. Stretching a surface in a rotating micropolar fluid. Int. Journal of science and technology, Spring Hall, pp: 30-36.
4. Shafique, M. and A. Rashid, 2006. Three dimensional micropolar flows due to a stretching flat surface. Int. J. of Math. Analysis, 1 (2): 173-187.
5. Able, S., P.H. Veena, K. Rajagopal and V.K. Pravin, 2004. Non- Newtonian magnetohydero dynamic flow over a stretching surface with heat and mass transfer. Int. J. Nonlinear Mech., 39: 1067-1078.
6. Asghar, S., K. Hanif, T. Hayat and C.M. Khalique, 2007. MHD non-Newtonian flow due to non coaxial rotations of an accelerated disk and a fluid at infinity. Communication in Nonlinear Sci. and Numerical Simulation, 12: 465-485.
7. Aldabe, N.T., E.F. Elshekawey Elsayed, M.E. Elbarbary and N.S. Elgazery, 2005. Chebyshev finite difference method for MHD flow of micropolar fluid past astretching sheet with heat transfer. Applied Mathematics and Computation, 160: 437-450.

8. Ishak, A., R. Nazar and I. Pop, 2008. Magneto hderodynamic flow of micropolar fluid towards a stagnation point on a vertical surface. Computers and Applications, 56: 3188-3194.
9. Hayat, T., T. Javed and Z. Abbas, 2009. MHD flow of micropolar fluid near a stagnation point towards a non linear stretching surface. Nonlinear Analysis: Real World Applications, 10: 1514-1526.
10. Sastry, V.U.K. and V.R.M. Rao, 1982. Numerical solution of micropolar fluid in a channel with porous walls. International Journal of Engineering Science, 20: 631-642.
11. Ashraf, M., M.A. Kamal and K.S. Syed, 2006. Numerical solution of steady viscous flow of a micropolar fluid driven by injection between two porous disks. Applied Mathematics and Computation, 179:1-10.
12. Guram, G.S. and M. Anwar, 1981. Micropolar flow due to a rotating disk with suction and injection. ZAMM, 61: 589-595.
13. Ashraf, M., M.A. Kamal and K.S. Syed, 2006. Numerical simulation of a micropolar fluid between a porous disk and a non-porous disk. Appl. Math. Modell, 33: 1933-1943.
14. Dash, G.C. and P.C. Tripathy, 1993. Hydromaganetic flow and heat transfer between two horizontal plates, both the plates being stretching sheets. Modelling, Measurement and Control, B, ASME Press, 51 (2): 51-64.
15. Rossow, V.J., 1958. Tech. Report, 1358, NASA.
16. Smith, G.D., 1979. Numerical Solution of Partial Differential Equation, Clarendon Press, Oxford.
17. Gerald, C.F., 1989. Applied Numerical Analysis, Addison-Wesley Pub. NY.
18. Milne, W.E., 1970. Numerical Solution of Differential Equation, Dover Pub.
19. Burden, R.L., 1985. Numerical Analysis, Prindle, Weber & Schmidt, Boston.